2024 International Conference on Electromagnetics in Advanced Applications (ICEAA) | 979-8-3503-6097-4/24/$31.00 ©2024 IEEE | DOI: 10.1109/ICEAA61917.2024.10701816

Method of Moments for the Two-Dimensional Analysis of Array-Fed Metasurface Antennas

Jonathan Dessy
ICTEAM institute
Université catholique de Louvain
Louvain-la-Neuve, Belgium
jonathan.dessy@uclouvain.be

Modeste Bodehou
EPAC
Université d'Abomey-Calavi
Abomey-Calavi, Benin
modeste.bodehou@gmail.com

Christophe Craeye
ICTEAM institute
Université catholique de Louvain
Louvain-la-Neuve, Belgium
christophe.craeye@uclouvain.be

***Abstract*—This paper presents a Method of Moment (MoM) formulation for the two-dimensional analysis of array-fed metasurface (MTS) antennas. In the considered problem, the MTS is only modulated along one direction and translationally invariant along the other one. The MoM is first formulated for the case of a MTS of finite length fed with an array of active elements, with no particular constraint on the feed spacing, nor on the weight associated with each element. Then, the methodology is particularized to the case of a periodic MTS fed with an infinite array of active elements of same amplitude, with constant feed spacing and linear phase shift between elements. In both cases, the implementation is closely analysed and simulation results are shown to cross-validate both approaches. It can be concluded that the implemented methodologies can provide very fast and accurate results.**

***Index Terms*—Metasurface (MTS), array, Method of Moments (MoM), periodic.**

I. Introduction

Metasurface (MTS) antennas consist of a grounded dielectric slab on which sub-wavelength metal patterns of varying size and orientation are printed [1]–[3]. A feeder is integrated inside the dielectric layer and generates a surface wave (SW) that propagates within the layer. This SW is progressively perturbed by the modulation of the MTS, which can produce a well-controlled radiation pattern by leaky-waves (LWs) [4], [5]. The analysis of MTS antennas is made difficult because of the many sub-wavelength details of its electrically large surface. To that aim, efficient numerical methods based on Maxwell's equation in their surface-integral form have been developed in the literature, such as the Method of Moments (MoM) [6], [7]. In this method, the MTS layer is accurately modeled as a spatially modulated sheet impedance lying on a grounded substrate [8]–[11]. The MoM has been widely exploited for the analysis of MTS antennas fed at a single point [5], [9], [11]. Recent works have also considered multiple feeds to improve the conversion efficiency of the antenna [3], or to create multiple beams [12], [13]. However, their number is always very limited (typically less than 10 feeds). In this paper, we propose to analyse MTS antennas fed with an array of several feeds within the dielectric slab, and with no constraint on the total number of feeds. We will mainly focus on their efficient numerical simulations. Such structures could offer new possibilities in the design of MTS antennas, such as providing beam scanning [13]. In particular, we are interested in structures that are modulated along one direction only, and infinitely invariant along the other direction, which corresponds to a two-dimensional (2D) problem. This type of MTSs will be named one-dimensional (1D) MTSs, and this paper will focus on their efficient analysis as they allow a first simplified and relevant analysis of array-fed MTS antennas. The methodology could then be extended to the study of more complex structures with 2D modulation. A special attention will be given to periodic MTSs, both at the feed and impedance sheet levels.

The paper is structured as follows. Section II describes the Method of Moments (MoM) formulation for the 2D analysis of 1D MTS antennas. Then, Section III shows and analyses simulation results obtained with the previously detailed codes. Finally, conclusions are drawn in Section IV.

II. Method of Moments

The MoM for the analysis of modulated MTS antennas has been well studied in the literature [5], [8]–[13]. It consists in determining the current distribution supported by the antenna for a given excitation and impedance model of the MTS. It is typically done by solving the electric field integral equation (EFIE) [8]. This section shows how the MoM formulation can be simplified for the case of 1D isotropic MTS antennas that are modulated only along the x direction, and infinitely invariant along y. The MTS has a finite length l along x, and is printed on an infinitely long dielectric slab of relative permittivity ϵ_r and thickness d_{slab}. Both layers are infinitely long and invariant along y. Each excitation is modeled as a wall (along y) of vertical elementary dipoles (VEDs) located in the middle of the substrate ($z = -d_{slab}/2$). A cut of the considered structure is shown in Fig. 1. In this particular case, the current distribution and the tangential electric field on the MTS are x-oriented. Thus, the EFIE simplifies to [14]:

$$\int_{x'} G^{xx}(x,x')\, J^x(x')\, dx' - Z_s(x)\, J^x(x) = -E_i^x(x) \quad (1)$$

where the x exponent refers to the x component of each vector. The incident electric field is denoted as E_i^x, J^x is the current distribution, G^{xx} is the Green's function of the grounded slab,

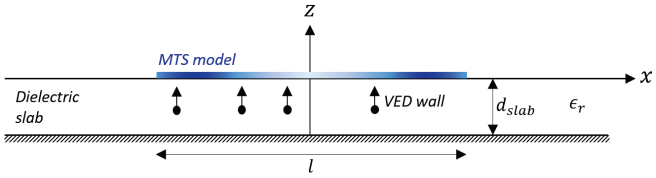

Fig. 1. 1D isotropic MTS antenna modulated along x. The MTS has a finite length l along x, and is infinitely invariant along y. Each excitation is modeled as a VED wall (along y).

Z_s is the isotropic surface sheet impedance model of the MTS, and x, x' refer to the positions of observation and source, respectively. In the MoM, the unknown current distribution is decomposed into a weighted sum of x-oriented basis functions:

$$J^x(x) = \sum_{n=1}^{N} i_n \; F_b^n(x) \tag{2}$$

where i_n is the weight associated with the n-th basis function F_b^n. In this work, the basis functions are chosen to be Gaussian functions [9]:

$$F_b^n(x) = \frac{1}{\sigma\sqrt{2\pi}} \; e^{\frac{-(x-\mu_n)^2}{2\sigma^2}} \tag{3}$$

where σ and μ_n denote the standard deviation and mean of the n-th basis function, respectively. Those parameters are chosen such that there are around 20 basis function per wavelength, and the basis functions cross each other around -1dB from their top. Their relatively local spatial behavior justifies their choice for representing the current. Those functions admit a closed form Fourier transform given by:

$$\tilde{F}_b^n(k_x) = e^{jk_x\mu_n} \; e^{\frac{-\sigma^2 k_x^2}{2}} \tag{4}$$

where k_x is the spectral coordinate. Inserting (2) in (1) and testing the fields with the same basis functions (Galerkin testing) allows one to build the MoM linear system of equations:

$$(\boldsymbol{Z_G} - \boldsymbol{Z_{IBC}}) \; \boldsymbol{i} = \boldsymbol{v} \tag{5}$$

where $\boldsymbol{Z_G}$ is the substrate matrix, $\boldsymbol{Z_{IBC}}$ is the impedance boundary condition (IBC) matrix, $\boldsymbol{i}$ is the vector containing the unknown current coefficients, and $\boldsymbol{v}$ is the excitation vector. It can be shown that their mathematical expressions read as:

$$Z_G(m,n) = \frac{1}{2\pi} \int_{k_x} \tilde{F}_t^m(-k_x) \; \tilde{G}^{xx}(k_x) \; \tilde{F}_b^n(k_x) \; dk_x \tag{6}$$

$$Z_{IBC}(m,n) = \int_x F_b^n(x) \; Z_s(x) \; F_t^m(x) \; dx \tag{7}$$

$$v(m) = \frac{-1}{2\pi} \int_{k_x} \tilde{E}_i(k_x) \; \tilde{F}_t^m(-k_x) \; dk_x \tag{8}$$

where F_t^n refers to the n-th testing function. Since the layered Green's functions [15], the incident electric field [16], and the basis and testing functions have analytical Fourier transforms, $\boldsymbol{Z_G}$ and $\boldsymbol{v}$ are computed in spectral domain. A path in complex k_x plane must be used for those integrations as the Green's functions and the excitation both contain poles in spectral domain [17]. Because of the choice of the basis and testing functions, the matrices $\boldsymbol{Z_{IBC}}$ and $\boldsymbol{Z_G}$ have symmetric and symmetric Toeplitz structures, respectively. This can be exploited to speed up the computation time for the matrix filling. Note that, given the Gaussian shape of the basis and testing functions, many entries of the IBC matrix will be negligible (sparse matrix). In practice, interactions between basis and testing functions centered sufficiently far apart should not be computed and can directly be set to zero, which speeds up the IBC matrix filling. If the impedance model of the MTS is periodic, many entries of the IBC matrix will be similar, which allows for an even faster evaluation of this matrix. Finally, note that any feeding law, such as an irregularly spaced and weighted array of VED walls within the dielectric slab, can be considered by simply adding the contribution of each VED wall to the incident electric field. Once the current distribution is found, the spectral electric field can be obtained as:

$$\tilde{E}^x(k_x) = \tilde{J}^x(k_x) \; \tilde{G}^{xx}(k_x) + \tilde{E}_i(k_x) \tag{9}$$

It is of interest to investigate the case of a periodic MTS fed with an array (along x) of VED walls of same amplitude with constant feed spacing a, but with linear phase shift $-\psi$ between consecutive elements. Since the MTS is supposed to be infinitely long, the MoM can be extended to the so-called periodic MoM developed for the analysis of infinitely periodic structures [18], [19]. In this case, the antenna can be seen as the infinite repetition of a reference cell and its corresponding reference feed, as shown in Fig. 2. Consequently, basis functions are only used on the reference cell and are implicitly repeated in the other cells with their appropriate phase shift, which drastically reduces the number of unknowns. Given the periodicity of the structure, spectral integrations are simplified into summations over Floquet wavenumbers, which speeds up the implementation and removes the need for the contour deformation. Their expressions are given by:

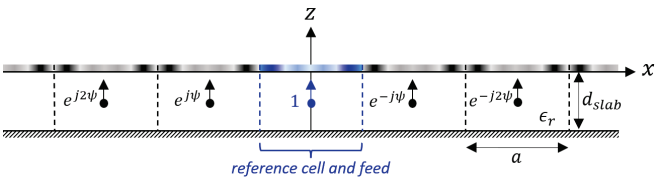

Fig. 2. 1D infinite isotropic periodic MTS antenna modulated along x. The reference cell and the corresponding reference feed are highlighted in blue.

$$Z_G(m,n) = \frac{1}{a} \sum_{p=-\infty}^{+\infty} \tilde{F}_t^m(-k_x^p) \; \tilde{G}^{xx}(k_x^p) \; \tilde{F}_b^n(k_x^p) \tag{10}$$

$$v(m) = \frac{-1}{a} \sum_{p=-\infty}^{+\infty} \tilde{E}_i(k_x^p) \; \tilde{F}_t^m(-k_x^p) \tag{11}$$

where k_x^p are the Floquet wavenumbers defined as:

$$k_x^p = \frac{\psi}{a} + p\frac{2\pi}{a} \tag{12}$$

Because of the sampling on the wavenumbers, the substrate matrix $\boldsymbol{Z_G}$ is no longer symmetric, but it keeps its Toeplitz structure. The IBC matrix computation is unchanged as it is computed in space domain, but one should keep in mind that the basis functions are implicitly repeated in consecutive cells, within a phase shift. Because of this repetition, the IBC matrix loses its symmetric structure. Note that, as the current and electric field are periodic in space domain, we know that their Fourier transform will be sampled, with sampling at the Floquet wavenumbers. In fact, we know from antenna array theory that the total radiation pattern will be the product between the array factor (AF), taking into account the effect of the array of excitations, and the embedded element pattern (EEP), which corresponds to the pattern of the antenna when only the reference feed is excited [20]. As the AF admits an analytical expression which simplifies into a Dirac comb for the case of an infinite array, it justifies the sampled aspect of the current and electric field. In general, one might be interested in obtaining the EEP of the infinite MTS to predict the behavior of the total pattern by multiplying it with the analytical expression of the AF. To that aim, paper [21] has shown that the unknown spectral current sampled at some specific Floquet modes $k_x^p = \psi/a + 2\pi p/a$ for excitation of the reference cell only, can be obtained from the spectral current of the structure when all cells are fed with consecutive phase shift $-\psi$ between cells. Thus, the implementation can rely on the previously explained periodic MoM code, which must be solved for many phase shifts to build the total spectral current. This current can be regarded as the superposition of many spectrally shifted Dirac combs [22]. As the MoM matrix depends on the imposed phase shift, it should be computed for every direction of observation. However, the substrate matrices for opposite phase shifts will be transposed, which can be exploited to speed up the implementation. In addition, one can save computation time by precomputing the IBC matrix interactions between the testing function (reference cell) and the basis functions in the reference cell and in (sufficiently close) other cells located at the left of the reference cell, and by saving all the results without applying any phase shift. Given the periodicity of the structure, interactions with basis functions to the right of the reference cell can be directly deduced from the previous computations. Then, whenever the periodic MoM is called, the IBC matrix can be evaluated very fast simply by multiplying the precomputed results with their corresponding phase shifts. As a last general comment, special attention must be given to the convergence of the integrations and summations for building the MoM linear system of equations. In particular, it is necessary to evaluate the required bounds and sampling rate for a fast and accurate computation of the integrals and summations.

III. Simulation Results

This section shows and analyses simulation results obtained with the previously detailed MoM codes. For all the simulations, we will consider an operating frequency of 24 GHz, and a dielectric slab of thickness $d_{slab} = 1.524$ mm and relative permittivity $\epsilon_r = 3.66$. The MTS sheet impedance modulation is given by:

$$Z_s(x) = jX_0\left(1 + M\sin\left(2\pi x/p\right)\right), \tag{13}$$

with $X_0 = -772.5\ \Omega$ the average impedance, $M = 0.4$ the modulation depth, and $p = \lambda/2$ the periodicity of the impedance, where λ is the free-space wavelength. First, a single excitation at the center of the antenna is considered to evaluate the impact of the MTS length. Then, examples of a MTS fed with a regular array of phase shifted elements of same amplitude is shown. Each of the following results has been obtained in less than one second on a conventional desktop computer.

A. Single excitation

Firstly, we consider a unique VED wall located in the center of the MTS ($x = 0, z = -d_{slab}/2$) and simulate the spectral electric field for different antenna lengths: $l = [10\lambda, 20\lambda, 100\lambda]$. Then, the periodic MoM code is used to predict the behavior of the spectral electric field if the length of the MTS is made infinite. Results are shown in Fig. 3. In all

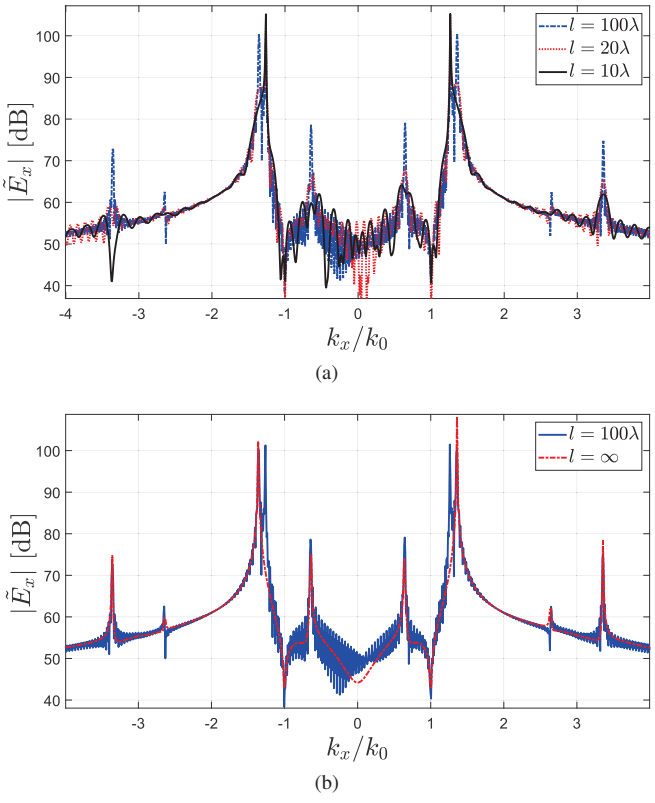

Fig. 3. Spectral electric field obtained with the impedance defined in (13) for different antenna lengths. (a) Finite MTS of length $l = [10\lambda, 20\lambda, 100\lambda]$. (b) Finite MTS of length $l = 100\lambda$, and infinite MTS.

curves of Fig. 3(a), we observe peaks which correspond to the main SW wavenumbers propagating in the MTS in the absence of modulation ($k_{sw} = \pm 1.35 k_0$) and their harmonics, as predicted by the theory [23]. As the length increases, currents and fields can propagate over a larger distance, resulting in

sharper patterns. Eventually, we observe in Fig. 3(b), that the pattern of a very long antenna converges to the one predicted by the infinite array, except for a slight mismatch between both curves due to the poles around $k_x = \pm 1.26 k_0$ in the case of a finite MTS. In fact, those poles are associated with the fields propagating in the structure beyond the finite MTS, in the infinite dielectric slab. This comparison contributes to cross-validating both MoM codes. Then, the spectral electric

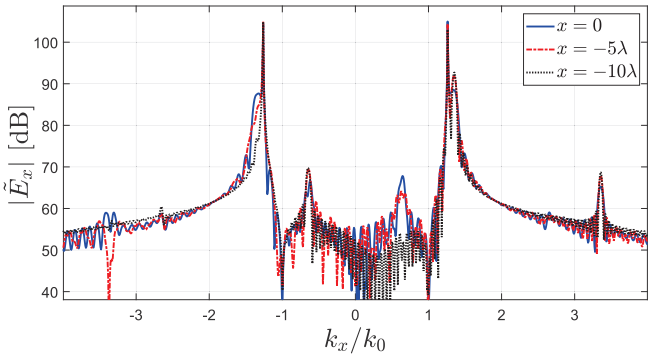

Fig. 4. Spectral electric field of a MTS of length $l = 20\lambda$ modulated with the impedance defined in (13), for different feed locations: $x = [-10\lambda, -5\lambda, 0]$.

field for the antenna of length $l = 20\lambda$ has been simulated for different feed locations: $x = [-10\lambda, -5\lambda, 0]$. Results are shown in Fig. 4. It can be observed that the prediction of infinite array becomes less valid for feeds located close to the edges of the antenna. In particular, we can understand that if the feed is in the left-side of the antenna, there is more current propagating to the right than to the left of the feed. So, the main positive SW wavenumber $(+k_{sw})$ as well as its harmonics have a greater impact in the final pattern than the main negative SW wavenumber $(-k_{sw})$ and its harmonics.

B. Array excitation

Secondly, we consider an antenna of length $l = 20\lambda$ with the same set of parameters as previously, but excited with an array of VED walls of same amplitude with feed spacing $a = p = \lambda/2$ and consecutive phase shift $-\psi$ between cells. There are 41 feeds in total, located at $x = [-10\lambda, -9.5\lambda, ..., 0, ..., 10\lambda]$. Results are shown in Fig. 5, for $\psi = [0, \pi/4]$. As expected, we observe peaks in the spectral currents located at the Floquet wavenumbers $k_x^p = \psi/a + p2\pi/a$. However, the peaks associated with $\pm k_{sw}$ and there harmonics are still present because of the edge effects. If the antenna length was infinite, the obtained spectral currents would be sampled at the corresponding Floquet wavenumbers.

IV. Conclusion

This paper has presented the MoM formulation for the 2D analysis of 1D MTS antennas. The methodology is very suitable to analyse any feeding network, where each excitation is modeled as an infinite wall (along y) of VEDs inside the dielectric layer. Because of the Gaussian shape of basis and testing functions, many numerical accelerations have been

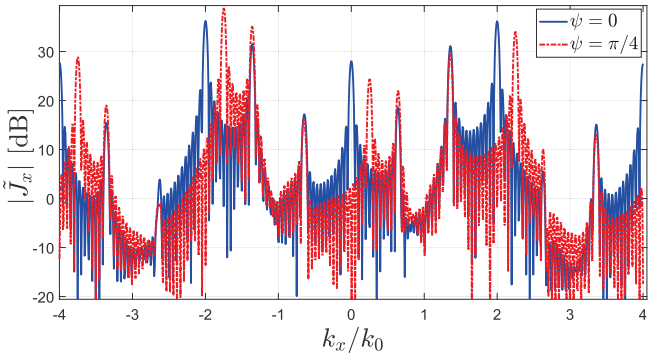

Fig. 5. Spectral current of a MTS of length $l = 20\lambda$ modulated with the impedance defined in (13), and fed with an array of 41 feeds of same amplitude with $a = p = \lambda/2$ and $\psi = [0, \pi/4]$.

considered. In particular, the formulation was adapted for the case of a periodic MTS fed with an array of VED walls of same amplitude with constant feed spacing a, and with linear phase shift $-\psi$ between consecutive elements. In this case, the periodicity can be exploited to simulate efficiently the response of the infinite array. Simulation results have shown that the spectral electric field obtained for a sufficiently long antenna converged to the one predicted by the infinite array, except for poles only present if the MTS is of finite length. In fact, those poles are associated with the fields propagating beyond the MTS, in the infinite dielectric slab. This comparison contributes to cross-validating both MoM codes. It can be concluded that the presented tools allow a very accurate and fast simulation of MTSs that are modulated along one direction only. The methodology can then be extended for the analysis of MTSs modulated along both directions.

Acknowledgment

Jonathan Dessy's activity is funded under a Research Fellowship of the Fonds de la Recherche Scientifique - FNRS.

References

[1] B. H. Fong, J. S. Colburn, J. J. Ottusch, J. L. Visher, and D. F. Sievenpiper, "Scalar and tensor holographic artificial impedance surfaces," *IEEE Trans. Antennas Propag.*, vol. 58, no. 10, pp. 3212–3221, Jul. 2010.

[2] G. Minatti, S. Maci, P. De Vita, A. Freni, and M. Sabbadini, "A circularly-polarized isoflux antenna based on anisotropic metasurface," *IEEE Trans. Antennas Propag.*, vol. 60, no. 11, pp. 4998–5009, Nov. 2012.

[3] M. Bodehou, A. Guth, K. A. Khalifeh, D. Heberling, and C. Craeye, "Multi-feed metasurface antennas: Direct numerical design and experimental validations," *IEEE Access*, vol. 11, pp. 35 754–35 762, Apr. 2023.

[4] G. Minatti, F. Caminita, E. Martini, M. Sabbadini, and S. Maci, "Synthesis of modulated-metasurface antennas with amplitude, phase, and polarization control," *IEEE Trans. Antennas Propag.*, vol. 64, no. 9, pp. 3907–3919, Sep. 2016.

[5] M. Bodehou, K. A. Khalifeh, S. N. Jha, and C. Craeye, "Direct numerical inversion methods for the design of surface wave-based metasurface antennas: Fundamentals, realizations, and perspectives," *IEEE Antennas Propag. Mag.*, vol. 64, no. 4, pp. 24–36, Aug. 2022.

[6] R. F. Harrington, "Field computation by moment methods," *Wiley-IEEE Press*, 1993.

[7] S. Rao, D. Wilton, and A. Glisson, "Electromagnetic scattering by surfaces of arbitrary shape," *IEEE Trans. Antennas Propag.*, vol. 30, no. 3, pp. 409–418, May 1982.

[8] M. A. Francavilla, E. Martini, S. Maci, and G. Vecchi, "On the numerical simulation of metasurfaces with impedance boundary condition integral equations," *IEEE Trans. Antennas Propag.*, vol. 63, no. 5, pp. 2153–2161, May 2015.
[9] D. González-Ovejero and S. Maci, "Gaussian ring basis functions for the analysis of modulated metasurface antennas," *IEEE Trans. Antennas Propag.*, vol. 63, no. 9, pp. 3982–3993, Sep. 2015.
[10] M. Bodehou, C. Craeye, H. Bui-Van, and I. Huynen, "Fourier–Bessel basis functions for the analysis of elliptical domain metasurface antennas," *IEEE Antennas Wireless Propag. Lett.*, vol. 17, no. 4, pp. 675–678, Apr. 2018.
[11] J. Cavillot, M. Bodehou, S. Hubert, and C. Craeye, "Efficient analysis of planar, arbitrarily shaped, and (bi)-anisotropic metasurface antennas," *IEEE Trans. Antennas Propag.*, vol. 70, no. 1, pp. 536–546, Jan. 2022.
[12] D. González-Ovejero, G. Minatti, G. Chattopadhyay, and S. Maci, "Multibeam by metasurface antennas," *IEEE Trans. Antennas Propag.*, vol. 65, no. 6, pp. 2923–2930, Jun. 2017.
[13] M. Bodehou, E. Martini, S. Maci, I. Huynen, and C. Craeye, "Multi-beam and beam scanning with modulated metasurfaces," *IEEE Trans. Antennas Propag.*, vol. 68, no. 3, pp. 1273–1281, Mar. 2020.
[14] J. Dessy, M. Bodehou, J. Cavillot, and C. Craeye, "Sparse-array metasurface for beam scanning," submitted to *IEEE Trans. Antennas Propag.*, Dec. 2023.
[15] N. Das and D. Pozar, "A generalized spectral-domain Green's function for multilayer dielectric substrates with application to multilayer transmission lines," *IEEE Trans. Microw. Theory Techn.*, vol. 35, no. 3, pp. 326–335, Mar. 1987.
[16] K. Michalski and J. Mosig, "Multilayered media green's functions in integral equation formulations," *IEEE Trans. Antennas and Propag.*, vol. 45, no. 3, pp. 508–519, Mar. 1997.
[17] A. Fort, F. Keshmiri, G. R. Crusats, C. Craeye, and C. Oestges, "A body area propagation model derived from fundamental principles: Analytical analysis and comparison with measurements," *IEEE Trans. Antennas Propag.*, vol. 58, no. 2, pp. 503–514, Feb. 2010.
[18] L. Trintinalia and H. Ling, "Integral equation modeling of multilayered doubly-periodic lossy structures using periodic boundary condition and a connection scheme," *IEEE Trans. Antennas Propag.*, vol. 52, no. 9, pp. 2253–2261, Sep. 2004.
[19] X. Dardenne and C. Craeye, "Method of moments simulation of infinitely periodic structures combining metal with connected dielectric objects," *IEEE Trans. Antennas and Propag.*, vol. 56, no. 8, pp. 2372–2380, Aug. 2008.
[20] C.A. Balanis, *Antenna Theory, Analysis and Design (3rd ed.)*, pp. 283-333, *John Wiley & Sons*, 2005.
[21] C. Craeye and D. Gonzalez Ovejero, "A review on array mutual coupling analysis," *Radio Science*, vol. 46, no. RS2012, p. 25, Apr. 2011.
[22] B. Munk and G. Burrell, "Plane-wave expansion for arrays of arbitrarily oriented piecewise linear elements and its application in determining the impedance of a single linear antenna in a lossy half-space," *IEEE Trans. Antennas Propag.*, vol. 27, no. 3, pp. 331–343, May 1979.
[23] A. Oliner and A. Hessel, "Guided waves on sinusoidally-modulated reactance surfaces," *IRE Trans. Antennas Propag.*, vol. 7, no. 5, pp. 201–208, Dec. 1959.